Geophys. J. R. astr. Soc. (1975) **43**, 307–326

Tidal Triggering of Earthquakes*

Thomas H. Heaton

(Received 1975 April 14)†

Summary

Analysis of the tidal stress tensor at the time of moderate to large earthquakes strongly suggests that shallow (<30 km) larger magnitude oblique-slip and dip-slip earthquakes are triggered by tidal stresses. No corresponding triggering effect is seen for shallow strike-slip earthquakes or for any type of intermediate or deep focus earthquakes which have been studied. Tidal triggering is also discussed from the viewpoint of the 'dilatancy-diffusion' model. Specifically, the model as usually stated, excludes the possibility of small earthquakes being tidally triggered.

Introduction

The study of tides provides a unique opportunity to view the response of the Earth to *known* changes in stress (known in the sense of an assumed model). The response of the Earth to these known stresses must limit our ideas of how the Earth responds to the much larger and generally unknown tectonic stresses which are ultimately responsible for earthquakes. The fact that practically any ultra-long period strain measurements of the Earth are dominated by the luni-solar tide indicates that although tidal stresses are probably at least three orders of magnitude smaller than the tectonic stresses upon which they are superimposed, *tidal stress rates* may be comparable to *tectonic stress rates.* Before discussing the possible effects of tides on earthquakes, a few basic facts about tides will be reviewed. Also included is a brief review of a few previous tidal triggering studies.

There are two types of tides which produce observable strains in the Earth's crust: solid earth tides and oceanic tides.

Solid earth tides

On a global scale, differential gravitational forces exerted by the Sun and Moon cause the surface of the Earth to yield radially by up to 40 cm. Since tidal periodicities are an order of magnitude longer than the longest period free oscillations of the Earth, the deformations caused by tides are usually modelled by equilibrium elasticity theory. Strains in the Earth's crust caused by tides can be directly computed from the vertical deformations and dimensionless constants of proportionality called Love and Shida numbers. The boundary condition of no traction acting on the Earth's surface

* Contribution No. 2566, Division of Geological and Planetary Sciences, California Institute of Technology, Pasadena, California 91125.

† Received in original form 1975 February 21.

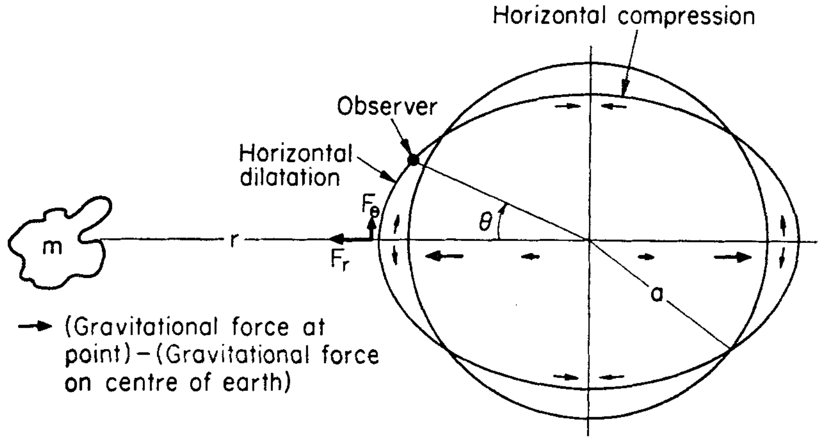

FIG 1. Schematic for tidal forces and deformation along any great circle passing directly beneath the mass.

$$\text{Tidal potential} \equiv W_2 = \frac{Gm}{2}\frac{a^2}{r^3}(3\cos^2\theta - 1)$$

$$F_\theta = -\frac{\partial W_2}{a\partial\theta} \qquad F_r = -\frac{\partial W_2}{\partial a}$$

$$u_r = \frac{h}{g}W_2 \qquad u_\theta = \frac{l}{g}\frac{\partial W_2}{\partial\theta}$$

$$e_{rr} = \frac{\partial u_r}{\partial r} \qquad e_{\theta\theta} = \frac{1}{r}\frac{\partial u_\theta}{\partial\theta} + \frac{u_r}{r}$$

G = universal gravitation constant, $6{\cdot}67 \times 10^{-8}$ dyne cm^2 g^{-2}

g = acceleration of gravity, 980 cm s^{-2}

$$\left.\begin{array}{l} h \approx 0{\cdot}6 \\ l \approx 0{\cdot}07 \end{array}\right\} \text{Love numbers}$$

yields the conclusion that tidal stresses normal to the free surface (provided the observer is at a sufficiently shallow depth) are zero. Thus for an observer near the Earth's surface, the minimum absolute principal stress axis is always vertical. Therefore, the remaining principal stress axes are in the horizontal plane and change their orientation as the tidal bulge moves around the Earth. A fairly involved argument is necessary to show that when the tide producing body is directly overhead, the Earth is stretched upward and the horizontal tidal stresses are tensile. When the tide producing body is on the horizon, horizontal tidal stresses are compressional (see Fig. 1). Tides are computed separately for the Moon and Sun and then combined; the lunar tides being about twice the amplitude of solar tides.

Oceanic tides

The effects of oceanic tides on crustal stresses are generally difficult to model. The free period of oceanic waves can be comparable to tidal periodicities and thus resonance phenomena cause oceanic tides to differ significantly from static equilibrium in both phase and amplitude. Oceanic tides sometimes depart from equilibrium by several metres, and are therefore capable of generating significant vertical and horizontal stresses (up to 0·3 bars on some coastal shelves). To model oceanic tidal effects on crustal stress then, one must first model oceanic tides and then model the response of the Earth to a complicated distribution of vertical forces. Modelling of this sort has been done (see Langdon & Thomas (33)), but due to the complexity of the problem, oceanic tides have been ignored for this study. In many instances one could argue that crustal shear stresses due to oceanic tides are small compared to the solid earth tides. These arguments are not always satisfactory and it seems clear that loading stresses from oceanic tides should be modelled to fully evaluate the effects of tides on earthquakes.

Earthquakes and tides

Suppose that earthquakes result from stress accumulations on the order of 150 bars. Suppose further that in active areas a fault would break once every 100 years. Although it is conceivable that the tectonic stress rate prior to failure is quite high, the tectonic stress rate averaged over the recurrence interval for such a region would be about 0·001 bars/6 hr. Tidal stress rates which can be 0·1 bars/6 hr are two orders of magnitude larger than this. Despite many attempts to solve the problem though, the question of whether tides trigger earthquakes is still unresolved. It is very difficult to disprove tidal triggering since it can always be contended that the wrong parameter or data set were used. Knopoff **(30)** cross correlated 9000 Southern California earthquakes of magnitude greater than 2 with the tidal potential. He found that the occurrence of earthquakes appeared random with respect to the tides. Studies of triggering of earthquakes on a worldwide basis have been done by Shlien **(58)** and Dix **(16)** among others. These studies appear to be inconclusive at best. There are also many papers supporting tidal triggering. Unfortunately, not all of these reports are consistent. Some have found that large earthquakes are more likely to be triggered than small ones (see Allen **(7)**, also Tamrazyan **(64)**), and yet there have been several positive correlations noted for microearthquake swarms. Ryall, Van Wormer & Jones **(52)** report a cross correlation coefficient which is significant at the 99 per cent confidence level for a swarm near Truckee, California. Willis & Taylor **(71)** reported correlations between Nevada microseismicity and tides. Caution is necessary using microearthquakes since the seismic noise level and hence the threshold for measuring microearthquakes often has a diurnal period due to manmade noise **(32)**.

There have also been reports of correlations between tides and volcanoes. Hamilton **(24)** and Mauk & Johnston **(38)** found tidal periodicities in volcanic eruptions. Some investigators have found that earthquakes are triggered during the maximum amplitude for tidal potential; others have found that earthquakes are triggered during maximum rate of change of amplitude; and still others have found that tides have nothing to do with earthquakes. In general, things seem confused. We are faced with the question: How might tides trigger earthquakes anyway? To answer this question, we must decide what might be important in determining when a rock breaks, and then decide how tides enter into our hypothetical fracture criteria.

Tidal stress and fault orientation

Although the parameters relevant to fracture may be a function of stress, time and constitutive law (which in the failure region may itself be a function of position and time), it seems clear that a complete time history of stress in the region of an earthquake would be a useful piece of information. This, of course, is not obtainable. However, variations in stress due to tides can be calculated. In most tidal triggering

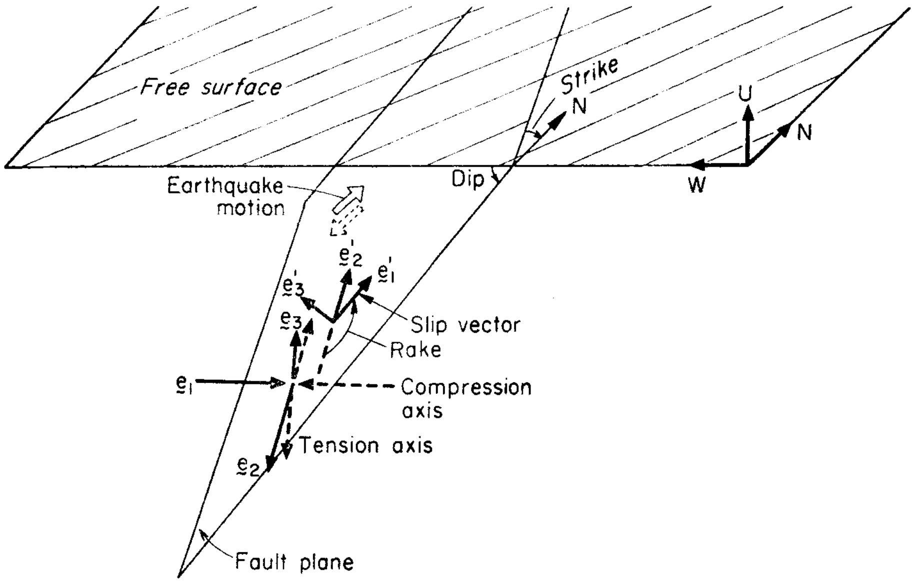

FIG. 2. Definition of co-ordinates systems ($\mathbf{e}_1$, $\mathbf{e}_2$, $\mathbf{e}_3$) and ($\mathbf{e}_1'$, $\mathbf{e}_2'$, $\mathbf{e}_3'$) for a thrust fault.

studies, only tidal potential has been considered. The relation between potential and stress state (and therefore earthquakes) is not always clear. Since the Sun and Moon traverse approximately the same trajectories each day, tidal stress cycles may essentially repeat themselves from one day to the next. If we confine ourselves to one nearly homogeneous local tectonic stress system and season, then earthquakes might occur at a consistent phase of the tides which can be characterized by the single parameter, tidal potential. When considering several different tectonic stress systems or seasons, special care must be taken to calculate how the tidal stresses relate to tectonic stresses.

Six independent variables are necessary to characterize the symmetric stress tensor at any point in the Earth. Assume the stress in the region of an earthquake to be the sum of the tectonic stress tensor, $\boldsymbol{\sigma}$ and the tidal stress tensor, $\boldsymbol{\tau}$. A fixed co-ordinate frame should be chosen in order to sum the tectonic and tidal stresses. For earthquake studies, the fault plane and slip vector of an earthquake can be utilized to define the most useful co-ordinate frames. First consider the frame ($\mathbf{e}_1$, $\mathbf{e}_2$, $\mathbf{e}_3$) defined by the maximum, intermediate, and minimum principal stress axes, respectively, which can be calculated from the known fault plane and slip vector (see Fig. 2). The tectonic stress tensor, $\boldsymbol{\sigma}$, is very nearly diagonal in this frame and for this study assume that $\boldsymbol{\sigma}$ is diagonal in the ($\mathbf{e}_1$, $\mathbf{e}_2$, $\mathbf{e}_3$) frame. This frame is very convenient since most fracture criteria for the fixed fault are easily expressed as functions of σ_{11}, σ_{22}, and σ_{33}. The shear stress causing the earthquake is simply $(\sigma_{11}-\sigma_{33})/2$. Unfortunately, the tidal stress tensor has no knowledge of the tectonic co-ordinate frame and in general it is not diagonal in the frame ($\mathbf{e}_1$, $\mathbf{e}_2$, $\mathbf{e}_3$). Yet by rotating the tidal stress tensor, $\boldsymbol{\tau}$, into this frame, some idea of how tides affect parameters such as deviatoric stress and confining pressure can be obtained in a co-ordinate system natural to the earthquake. Since $\boldsymbol{\tau}$ is not diagonal in the ($\mathbf{e}_1$, $\mathbf{e}_2$, $\mathbf{e}_3$) frame, the tidal shear stress acting on the rupture surface is not generally equal to $(\tau_{11}-\tau_{33})/2$. For this reason it is convenient to introduce a second co-ordinate frame ($\mathbf{e}_1'$, $\mathbf{e}_2'$, $\mathbf{e}_3'$) (see Fig. 2), where $\mathbf{e}_1'$ is parallel to the slip vector and $\mathbf{e}_3'$ is perpendicular to the fault plane. In this frame, τ'_{13} is the actual tidal shear stress sympathetic to failure.

Taking the epicentral location, the directions and distances of the Sun and Moon were computed as a function of time using standard theory of planetary motion and the Ile lunar theory. Computer programs written by Henry Fliegel of the Jet Propulsion Laboratory were used to make these calculations. Takeuchi's (63) work was then used in a computer program written by Hewitt Dix to calculate the Sun and Moon tidal stress tensors at the hypocentral location. The stress tensors were given relative to spherical polar co-ordinates with axes centred at the Earth's centre and polar axis towards the Sun or Moon. The stress tensors thus found were then referred to rectangular co-ordinates (up, south, east) with origins at the focus. The stress tensors were then added and the resultant rotated into the primed and unprimed co-ordinate systems defined by the fault plane and slip vector of the earthquake. Due to the symmetry of the stress tensor, either of the two complementary fault planes and slip vectors which are obtained from the fault plane solution give sufficient information to rotate the tidal stress tensor into the co-ordinate systems defined above. Various functions of $\tau(t)$ and $\tau'(t)$ were investigated (i.e. different failure criteria), to discover whether the origin times of earthquakes had any simple dependence upon tidal stresses.

Choice of earthquake sample

The major purpose of this study is to determine if the time at which an earthquake occurs depends upon tidal stresses. It seems clear that to optimize any possible tidal effects, only earthquakes whose origin time is independent of other obvious factors should be chosen. For instance, the origin times for earthquakes which belong to a closely-spaced sequence (e.g. foreshock–aftershock sequence) are probably not independent of one another. There was an attempt made then to use only large mainshocks which were not preceded by foreshocks. The fault plane and slip vector for each quake should be known and well constrained. These parameters were obtained from either observed surface rupture or seismically determined fault plane solutions. Because of the free surface boundary condition on earth tides, τ'_{31} (the shear stress sympathetic to failure) for dip-slip earthquakes on vertical faults is always nearly zero. Thus the polarity of the tidal shear stress for such an earthquake is always sensitive to minor errors in the fault plane solution. For this reason, vertically

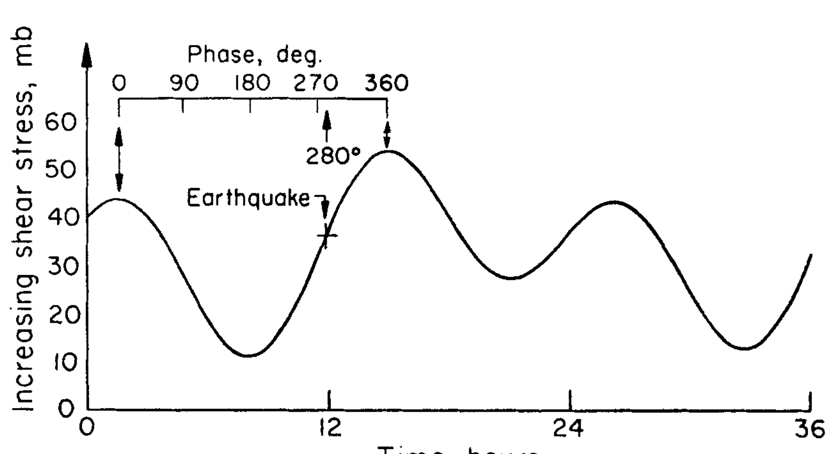

FIG. 3. Example showing how earthquakes were assigned a phase relative to the tides.

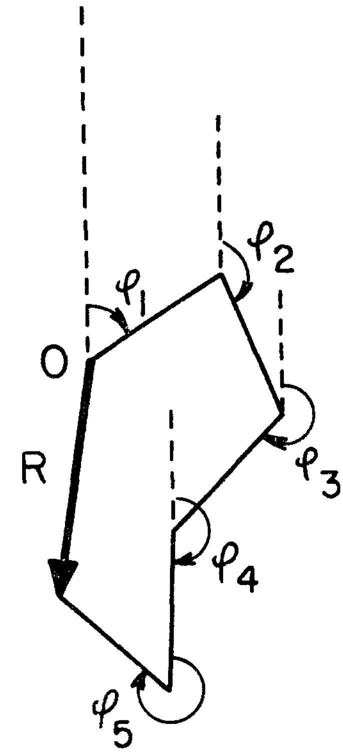

FIG. 4. Geometric interpretation of P_R. P_R is the probability that a random walk consisting of m unit steps will walk a distance of R or greater.

$$R = \sqrt{\left(\left(\sum_{i=1}^{m} \sin \rho_i\right)^2 + \left(\sum_{i=1}^{m} \cos \rho_i\right)^2\right)} \qquad P_R \approx \exp\left(-\frac{R^2}{m}\right).$$

faulted dip-slip earthquakes were not considered. Earthquakes which appeared to meet the specifications given above were rather randomly chosen from many different sources. The earthquakes were then classified according to depth, type of mechanism, location, etc. Clearly, judgment was required in deciding which earthquakes to include and how to classify them. To protect against systematic error due to my own prejudices, the decisions were made about the earthquakes before any tides were computed and furthermore the decisions were final.

Data analysis

Various components and combinations of components of τ and τ' were plotted as a function of time. Each earthquake was assigned a phase on a linear scale from 0° to 360°, where 0° was maximum tidal stress directly before the earthquake and 360° was the maximum tidal stress directly after the earthquake (see Fig. 3). These phases were then plotted on rose diagrams. A clustering of earthquake phases on the rose diagrams indicates a possible relation between tidal-stress and earthquakes. If earthquake origin times and tides are independent then the distribution of phases on the rose diagrams should appear uniform. A simple method for determining the degree of order in a rose diagram was developed by Rayleigh (**49**). Consider a two-dimensional vector in polar co-ordinates $u = (r, \phi)$ (see Fig. 4). If the magnitude of the vector sum of n unit 2-dimensional vectors $(1, \phi_i)$, is denoted by R and the ϕ_i correspond to earthquake phases then the probability, P_R, that a random set of n phases will produce a sum vector whose magnitude exceeds R is approximately equal to $\exp(-R^2/n)$. This approximation is sufficient when n is larger than 10. Thus the smaller P_R gets, the higher our confidence in tidal triggering becomes. Some caution should be used in interpreting P_R. Since the data sample has been grouped in many ways, the probability of finding a random sample with a small P_R is significant. For example, the probability of being dealt a flush in poker is small for any individual deal, but the probability of achieving a flush at some point during a long evening of poker is not so bad.

Results

A total of 107 earthquakes were included in the data sample and they appear in Table 1. They are grouped according to depth and focal mechanism. Earthquakes with depths listed as 33 km may have had the depth constrained. Rake is defined to be such that 0° is left-lateral movement and +90° indicates thrusting. Listed are the phases of both the tidal hydrostatic stress and tidal shear stress sympathetic to failure. Other stress parameters were investigated, but the best correlation obtained was with the shear stress, τ'_{13}. The hydrostatic stress $(\tau_{11}+\tau_{22}+\tau_{33})/3$, is proportional to the magnitude of the tidal potential and is independent of the co-ordinate frame. A comparison of the phases of the tidal hydrostatic stress and the phases of the tidal shear stress, τ'_{13}, thus gives an indication of the importance of orienting the tidal stress tensor relative to the motion of the earthquake. Figs 5 and 6 summarize the correlation of the phases of tidal stress with several different groupings of the earthquake sample. Fig. 5(a) shows no apparent correlation ($P_R = 0{\cdot}56$) between the phase of the tidal hydrostatic stress and the occurrence time of the earthquake. The correlation improved ($P_R = 0{\cdot}059$) when the phases of the sympathetic tidal shear stress were considered as is shown in Fig. 5(b). The possible correlation shown in Fig. 5(b) is evidently not due to earthquakes deeper than 30 km as Fig. 5(c) and (d) indicate no significant correlation of either hydrostatic ($P_R = 0{\cdot}26$) or shear stress ($P_R = 0{\cdot}15$) with origin time. Fig. 6(a) shows no significant correlation ($P_R = 0{\cdot}76$) between tidal shear stress and shallow strike-slip earthquakes. Fig. 6(b) and (c) illustrate that most of the possible correlation between all 107 earthquakes and tidal shear stress is due to that portion of the sample consisting of shallow (less than 30 km) dip-slip or oblique-slip earthquakes (greater than 30 per cent vertical motion). The phases of the hydrostatic stress for shallow dip-slip or oblique-slip events appear to be random ($P_R = 0{\cdot}77$), but the phases of the shear stress show a rather impressive correlation with origin times ($P_R = 1{\cdot}0 \times 10^{-5}$). Apparently, depth is an important parameter since dip-slip events in the 30 km to 50 km ($P_R = 0{\cdot}26$) region (see Fig. 6(d)) do not reflect the correlation seen for shallow events. This classification may be somewhat misleading, though, as earthquakes which are assigned depths of 33 km may well have been shallower.

Discussion

Although a larger data sample is desirable, some preliminary conclusions can be drawn from the results given above. Origin times for shallow dip-slip or oblique-slip earthquakes with magnitude greater than five appear to correlate strongly with tidal shear stresses acting sympathetic to failure. No corresponding correlation is found for shallow strike-slip earthquakes or for any earthquakes deeper than 30 km. Obviously, these conclusions do not give sufficient information to construct a model of failure. They do, however, provide constraints on any models which might be proposed. Let

Table 1

Ref.	Date	Origin time GCT	Comments	Magnitude	Depth (km)	Long. (deg)	Lat. (deg)	Strike (deg)	Dip (deg)	Rake (deg)	Phase of hydrostatic (deg)	Phase of shear (deg)
Earthquakes deeper than 50 km												
(25)	1963 September 17	05:54	Peru–Chile	6–3/4	76	78·2 W	10·6 S	N 5 W	35 W	−75	26	26
(25)	1963 September 24	16:30	Peru–Chile	6–1/2	60	78·3 W	10·7 S	N50 W	10 W	−90	216	208
(25)	1964 November 2	06:50	Peru–Chile	6–3/4	91	76·9 W	4·1 S	N30 W	30 W	−90	68	75
(25)	1964 November 28	16:41	Peru–Chile	5–1/2	650	71·3 W	7·9 S	N25 W	45 W	−85	115	115
(62)	1964 December 9	13:35	Chile	5·9	586	63·2 W	27·5 S	N10 W	80 W	−120	172	250
(25)	1965 March 5	14:32	Peru–Chile	5·6	573	63·3 W	27 S	N10 W	70 W	−110	273	339
(25)	1965 June 12	18:50	Peru Chile	5·8	102	69·3 W	20·5 S	N30 W	7 W	−90	83	61
(25)	1965 November 3	01:39	Peru–Chile	6·2	593	71·4 W	9·1 S	N10 W	50 W	−90	4	27
(25)	1966 May 1	16:22	Peru–Chile	5·8	154	74·3 W	8·4 S	N15 E	70 E	−115	31	3
(25)	1966 December 20	12:26	Peru–Chile	5·7	586	63·2 W	26·2 S	N20 W	70 W	−75	52	107
(25)	1967 January 17	01:08	Peru–Chile	5–1/2	590	63·3 W	27·4 S	N25 W	65 W	−115	145	288
(25)	1967 February 15	16:11	Peru–Chile	6·2	597	71·3 W	9 S	N10 W	45 W	−90	238	229
(62)	1967 May 11	15:05	Chile	6·1	115	68·5 W	20·3 S	N30 W	70 E	−100	283	265
(25)	1967 December 25	10:41	Peru–Chile	5·8	135	68·3 W	21·2 S	N20 W	25 W	−85	334	349
(25)	1967 December 27	09:17	Peru–Chile	6·4	135	68·3 W	21·2 S	N20 W	25 W	−85	218	212
(62)	1968 August 23	22:36	Chile	5·8	537	63·5 W	22 S	N 5 E	30 W	−80	180	141
(62)	1970 June 11	06:02	Chile	6·0	112	68·5 W	24·5 S	N10 W	25 W	−80	241	230
(62)	1970 June 19	10:56	Chile	6·3	52	70·5 W	22·2 S	N 5 W	70 E	−90	189	178
(43)	1970 July 31	17:08	Columbia	7·1	651	72·6 W	1·5 S	N20 W	30 E	−80	35	60
(25)	1964 July 9	16:39	New Hebrides	7–1/2	121	167·6 E	15·5 S	N 5 W	53 W	90	109	309
(25)	1966 June 13	18:08	New Hebrides	6	259	167·1 E	12·2 S	N10 E	45 W	55	256	64
(25)	1966 December 1	04:56	New Hebrides	6	132	167·1 E	14 S	N15 W	45 W	95	70	260
(25)	1966 December 21	08:52	New Hebrides	5·8	249	169·7 E	20 S	N15 E	65 E	−40	3	346
(25)	1967 January 19	12:38	New Hebrides	5·5	156	166·4 E	11·8 S	N 0	60 E	100	158	316
(25)	1967 March 31	20:05	New Hebrides	5·3	132	167·5 E	15·4 S	N15 W	45 W	90	107	308
(25)	1964 January 14	15:58	Solomons	5·6	169	150·8 E	5·2 S	N55 E	80 SE	90	52	210
(25)	1964 August 13	00:31	Solomons	6–1/2	392	154·3 E	5·5 S	N45 W	30 NW	−100	220	210
(25)	1966 August 5	04:33	Solomons	5·5	52	162·6 E	11·1 S	N50 W	45 NW	100	38	220
(25)	1966 December 14	21:07	Solomons	5·7	80	144·1 E	4·9 S	N50 W	60 NE	90	150	327
(25)	1968 January 7	09:56	Solomons	5·1	118	153·9 E	5·1 S	N35 W	45 NW	80	72	260
(25)	1965 April 29	15:28	NW United States	6–1/2	59	122·3 W	47·4 N	N10 W	70 E	−75	246	197

Table 1 (*continued*)

(14)	1966 June 6	07:46	Afghanistan	6–1/2	225	17·1 E	36·3 N	N90 W	40 N	92	315	135
(14)	1967 May 21	18:45	Sumatra	6·3	173	101·5 E	1 S	N20 W	70 W	120	81	281
(25)	1967 August 13	20:06	Honshu	6·0	357	135·E	35·3 N	N45 E	70 NW	−115	140	162
(14)	1969 January 19	07:02	Hokkaido	6–1/2	204	143·2 E	45 N	N30 W	88 W	45	125	60
Earthquakes between 30 and 50 km												
(19)	1940 August 1	15:08	Shakotan	7·0	33	139·5 E	44·4 N	N 0	46 E	90	50	220
(40)	1963 July 9	05:45	Mediterranean	5·5	33	8·2 E	43·4 N	N 2 E	40 E	80	217	317
(40)	1963 September 18	16:58	Mediterranean	5·2	33	29·2 E	40·9 N	N84 W	70 N	−100	194	179
(14)	1963 October 17	00:48	North Atlantic	6–1/4	33	37·4 W	7·6 N	N 5 W	85 E	5	295	261
(14)	1966 June 27	10:41	Nepal	6–1/2	37	80·9 E	29·7 N	N 45 W	25 NE	85	235	55
(1)	1966 October 17	21:42	Peru	7·5	38	78·6 W	10·7 S	N30 W	12 NE	90	71	300
(40)	1967 March 4	17:58	Mediterranean		33	24·6 E	39·2 N	N82 W	54 S	105	172	290
(14)	1969 February 3	21:41	Talaud	6–1/2	33	127·4 E	4·9 N	N30 W	60 SW	60	170	340
(1)	1970 May 31	20:23	Peru	7·8	43	78·2 W	9·2 S	N20 W	37 W	−90	151	150
(57)	1973 June 17	03:55	Japan	7·4	49	145·8 E	43 N	N50 E	27 NW	100	27	227
Shallow strike-slip earthquakes												
(36)	1836 June 10	15:30	Hayward (questionable)	7+	10	123 W	38 N	N35 W	90	180	285	80
(34)	1857 January 9	15:30	Ft Tejon	8+	10	117·5 W	34·5 N	N35 W	90	180	300	75
(34)	1865 September 9	20:30	San Andreas	7+	10	123 W	38 N	N35 W	90	180	320	95
(34)	1868 October 21	15:47	Hayward	7+	10	123 W	38 N	N35 W	90	180	115	255
(34)	1906 April 18	13:12	San Francisco	8+	10	123 W	38 N	N35 W	90	180	220	18
(50)	1932 December 21	06:10	Nevada (questionable)	7·3	10	118 W	34 N	N21 W	90	180	120	180
(50)	1933 August 11	01:54	Long Beach	6·3	8	118 W	33·6 N	N40 W	90	180	200	20
(50)	1940 May 19	04:37	Imperial Valley	7	8	115·5 W	32·7 N	N30 W	90	180	295	95
(50)	1947 April 10	15:58	Mannix	6–1/2	8	116 W	35 N	N30 W	90	180	170	325
(51)	1948 December 5	23:43	Desert Hot Springs	6–1/2	8	116·4 W	33·9 N	N54 W	60 NE	165	40	230
(13)	1966 June 28	04:26	Parkfield	6	9	121 W	37 N	N33 W	90	180	330	188
(6)	1968 April 9	02:29	Borrego Mtn	6–1/2	11	116 W	33 N	N48 W	83 NE	175	265	89
(15)	1969 October 2	04:56	Santa Rosa	5·9	10	122·6 W	38·5 N	N20 W	90	180	65	335
(28)	1927 March 7	09:27	Tango	7·9	8	134·3 E	35·3 N	N25 W	90	0	140	98

Table 1 *(continued)*

Ref.	Date	Origin time GCT	Comments	Magnitude	Depth (km)	Long. (deg)	Lat. (deg)	Strike (deg)	Dip (deg)	Rake (deg)	Phase of hydrostatic (deg)	Phase of shear (deg)
(28)	1943 September 10	08:37	Tottori	7·4	20	134 E	36 N	N80 E	90	180	235	165
(28)	1948 June 28	07:13	Fukui	7·3	10	136 E	36 N	N15 W	90	0	340	315
(44)	1969 September 9	05:15	Gifu	6–1/2	5	137 E	36 N	N30 W	90	0	110	80
(8)	1939 December 26	23:57	Anatolian Fault	8	10	39·7 E	39·7 N	N65 W	90	180	67	279
(8)	1943 December 20	14:03	Anatolian Fault	7·3	10	36·6 E	50·7 N	N65 W	90	180	166	36
(8)	1944 February 1	03:22	Anatolian Fault	7·3	10	33 E	41 N	N80 E	90	180	339	322
(8)	1953 September 7	19:06	Anatolian Fault	7·4	10	27·5 E	40 N	N70 E	90	180	275	228
(8)	1957 May 26	06:33	Anatolian Fault	7·1	10	31·2 E	40·6 N	N90	90	180	316	221
(40)	1965 March 9	17:57	Mediterranean	5·7	18	24 E	39·4 N	N40 E	90	180	138	123
(8)	1966 August 19	12:22	Anatolian Fault	6·8	10	41·6 E	39·2 N	N65 W	90	180	34	255
(8)	1967 July 22	16:52	Anatolian Fault	7·1	10	30·8 E	40·7 N	N90	90	180	189	88
(4)	1968 August 31	10:48	Khorasan	7·2	12	58·7 E	34 N	N90	90	0	290	170
(5)	1972 December 23	06:29	Nicaragua	6·0	5	86·3 W	12·1 N	N45 W	90	0	320	339
(45)	1973 March 17	08:30	Phillipines	7·0	10	122·8 E	13·4 N	N40 W	90	0	166	162
Shallow oblique-slip and dip-slip earthquakes												
(50)	1872 March 26	10:30?	Owens Valley	8+	8	117·5 W	34 N	N10 W	50 E	−110	60	65
(50)	1915 October 3	06:53	Nevada	7·6	8	117·5 W	40·5 N	N 0	54 E	−90	75	50
(50)	1934 January 30	18:16	Nevada	6·5	8	118·5 W	38 N	N65 W	73 N	−90	305	310
(50)	1946 March 15	13:49	Walker Pass (questionable)	6–1/4	8	118·1 W	35·7 N	N50 E	62 SE	55	215	55
(23)	1952 July 21	12:25	Kern County	7·7	10	119 W	35 N	N50 E	62 SE	55	135	305
(50)	1954 July 6	11:13	Nevada	6·6	8	118·5 W	38 N	N10 W	60 W	−90	10	15
(50)	1954 August 24	05:51	Nevada	6·8	8	118·3 W	38 N	N10 W	60 W	−90	20	10
(50)	1954 December 16	11:07	Nevada	7·1	8	118·3 W	39·5 N	N10 W	60 W	−90	275	280
(70)	1959 August 18	06:37	Montana	7·1	10	111 W	44·9 N	N80 W	54 S	−90	341	341
*	1970 September 12	14:30	Lytle Creek	5·4	10	118 W	34 N	N47 W	56 NE	54	240	18
(68)	1971 February 9	14:03	San Fernando	6–1/2	10	118·5 W	34 N	N64 W	52 NE	60	198	30
(17)	1973 February 21	14:30	Pt Mugu	5–3/4	18	119 W	34 N	N61 E	40 NW	56	85	315
(17)	1973 August 6	23:29	Anacapa	4·7	15	119 W	34 N	N90	70 S	20	305	50
(28)	1923 September 1	02:58	Kanto	8·2	30	140 E	35 N	N70 W	34 N	135	269	98

* Carl Newton, private communication.

Table 1 (*continued*)

(26)	1933 March 2	17:31	Sanriku	8–1/2	20	144·4 E	39·3 N	N 0	45 W	−90	345	350
(28)	1944 December 7	04:35	Tonankai	8	25	136 E	34 N	N35 E	15 NW	90	230	89
(28)	1946 December 20	19:19	Nankaido	8·2	25	136 E	34 N	N35 E	15 NW	90	190	35
(19)	1964 May 7	07:58	Oga	6·9	22	139 E	40·4 N	N30 E	40 NW	90	232	66
(28)	1964 June 16	04:01	Niigata	7·4	20	139 E	39 N	N15 E	65 W	90	221	20
(5)	1965 July 25	13:33	Japan	5·9	16	146·6 E	41·3 N	N45 E	45 NW	−105	37	42
(27)	1968 May 16	00·48	Tokachi-Oki	8	15	143·2 E	40·8 N	N24 W	20 W	35	250	295
(19)	1971 September 5	18:35	Sakhalin	7·1	22	141·2 E	46·5 N	N 4 E	52 W	90	110	294
(40)	1964 October 6	14:31	Mediterranean	6	10	24 E	39 ·4 N	N58 W	36 SW	−90	105	93
(40)	1965 July 6	03:18	Mediterranean	5·9	20	22·4 E	38·4 N	N87 E	76 S	−90	352	336
(40)	1966 February 5	02:02	Mediterranean	5·6	22	21·7 E	39·1 N	N46 W	46 SW	−55	106	95
(48)	1966 September 18	20:43	Iran	6·2	16	54·3 E	27·8 N	N45 W	45 SW	90	306	105
(40)	1967 May 1	07:09	Mediterranean	5·6	15	21·3 E	39·7 N	N 4 E	52 W	−70	37	44
(40)	1969 February 28	02:40	Mediterranean	7·3	22	10·6 W	36 N	N80 E	40 N	90	115	321
(65)	1970 March 28	21:02	Gediz	7	10	29·5 E	39 N	N10 W	60 E	−80	245	288
(61)	1964 March 28	03:36	Alaska	8–1/2	20	147·4 W	61·1 N	N63 E	10 SE	90	165	25
(2)	1965 March 30	02:37	Rat Island	7–1/2	20	177 ·9 E	50·3 N	N80 W	60 S	−90	111	104
(3)	1968 May 23	17:24	Inangahua (N.Z.)	7·1	21	171·9 E	41·7 S	N 0	45 E	90	202	49
(21)	1968 October 14	02:14	Meckering	6·9	5	117 E	31·8 S	N 0	45 E	105	77	263
(18)	1969 February 28	02:41	Portugal	7·9	22	10·6 W	36 N	N85 E	40 S	100	113	331

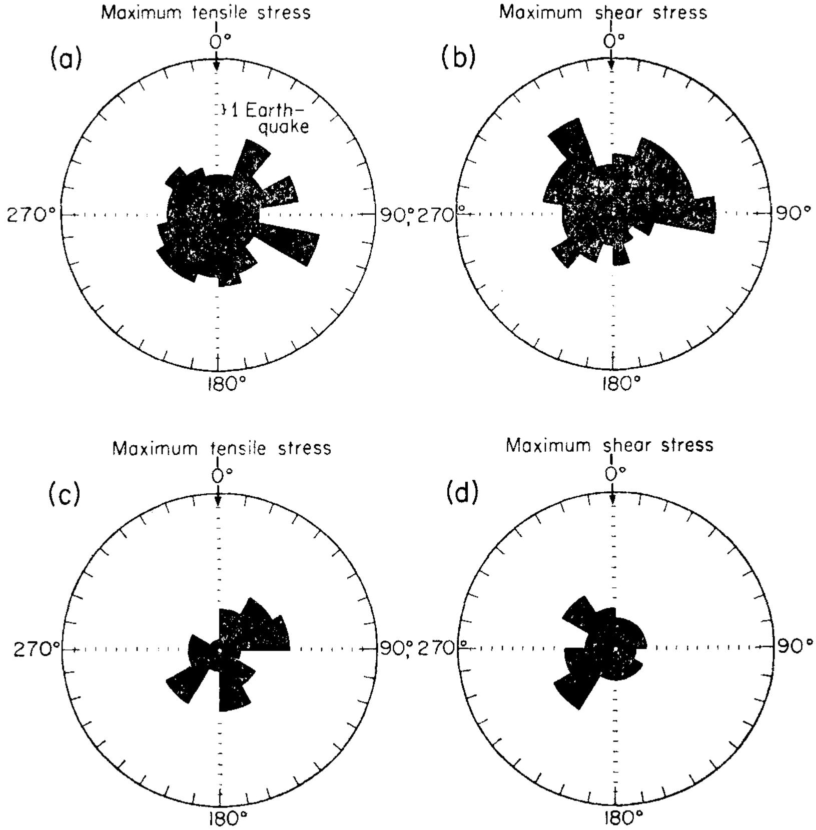

FIG. 5. Tidal phases for various groupings of the earthquake sample. (a) phases of tidal hydrostatic stress for all 107 earthquakes; $P_R = 0{\cdot}56$, (b) phases of tidal shear stress (τ'_{13}) for all 107 earthquakes; $P_R = 0{\cdot}06$, (c) phases of tidal hydrostatic stress for all earthquakes (45) deeper than 30 km; $P_R = 0{\cdot}26$, (d) phases (tidal) of shear stress for all earthquakes (45) deeper than 30 km; $P_R = 0{\cdot}15$.

us first consider the implications of the positive correlation found with shallow oblique-slip and dip-slip events.

(i) If it is true that tidal stress whose rate is of the order of 0·1 bars/6 hr affects the initiation of earthquake failure, this would imply that the rate of tectonic stress build up prior to the earthquake does not substantially exceed 0·1 bars/day. This is not too surprising since earthquakes with foreshocks were not considered and thus slowly changing stresses are reasonable. This stress-rate argument bears on the ' dilatancy-fluid diffusion ' model of earthquakes and will be discussed later.

(ii) The failure criterion, which is some functional of stress, a constitutive law, and time, is evidently sensitive to small perturbations in stress. This restricts the class of possible failure processes to those which, in some vague sense, are brittle for time periods on the order of 12 hr.

(iii) Although the true failure criterion is not known, it evidently is not independent of the shear stress. This may seem a statement of the obvious, yet some results from rock mechanics suggest that failure is most sensitive to confining pressure once sufficient shear stress is present.

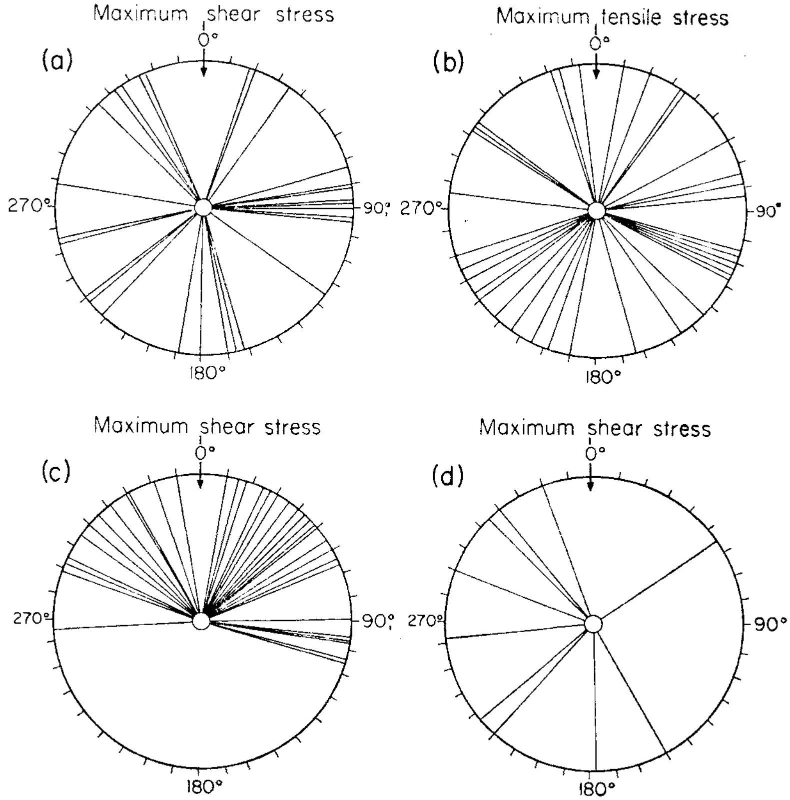

FIG. 6. Tidal phases for various groupings of shallow earthquakes. (a) phases of tidal shear stress for 28 shallow (less than 30 km) earthquakes with strike-slip motion; $P_R = 0{\cdot}76$, (b) phases of tidal hydrostatic stress for 34 shallow (less than 30 km) earthquakes with dip-slip or oblique motion; $P_R = 0{\cdot}77$, (c) phases of tidal shear stress for 34 shallow (less than 30 km) earthquakes with dip-slip or oblique-slip motion; $P_R = 1{\cdot}0 \times 10^{-5}$, (d) phases of tidal shear stress for 10 earthquakes between 30 and 50 km deep (1 strike-slip); $P_R = 0{\cdot}26$.

The implications of the absence of a correlation of the phases of the tidal shear stress with origin times for strike-slip and deep earthquakes are even more vague. Two explanations seem likely.

(i) The rate of tectonic stress build up is rapid just prior to the earthquake. This could be caused by rapid pore pressure changes or by other premonitory effects such as creep near the failure region.

(ii) The strength of the material has an important time dependence. That is, once the failure process is initiated, the rock will fail in some given time, regardless of small perturbations in stress.

It is important to recognize that a very simplified model of tidal triggering has been assumed in this study. Changes in the observed correlations would be anticipated if more realistic models of tidal stresses and failure processes were considered. Oceanic tidal loading, which would affect both the phase and character of the tidal stresses, has been ignored. Also, the shear stress is probably a crude approximation to the true fracture criterion and thus some other functional of the stress tensor may work better. Finally, other methods for assigning the phase of an earthquake with respect to the tides may give better results. The method used in this study, while statistically valid, presents a problem with causality. The peak in the tidal stress parameter *after* the earthquake is used to define the 360° point on the linear phase scale. How the origin time of an event should depend upon the nature of the stress after the event has occurred is not clear.

Tidal triggering and dilatancy-diffusion

The most important predictions of the dilatancy-diffusion model of earthquakes are that: (i) rocks strain non-linearly prior to an earthquake, (ii) the time period of anomalistic seismic velocity associated with an earthquake is an exponential function of the magnitude of the ensuing earthquake **(9, 54)**. When earth tides are incorporated into such a model, several interesting conclusions result.

(i) *Changes in observational Love numbers*

Beaumont & Berger **(11)** have discussed the problem of tidal strains in a dilatant region at some length. Their calculations indicate that changes of up to 60 per cent in the amplitude of observed tidal strains should occur near a dilatant region. My calculations indicate that due to non-linearity of a dilatancy constitutive law, changes in the character of the tidal strains should occur. Using experimental curves given by Brace **(12)** a non-linear elastic ' dilatancy-regime ' constitutive law has been developed

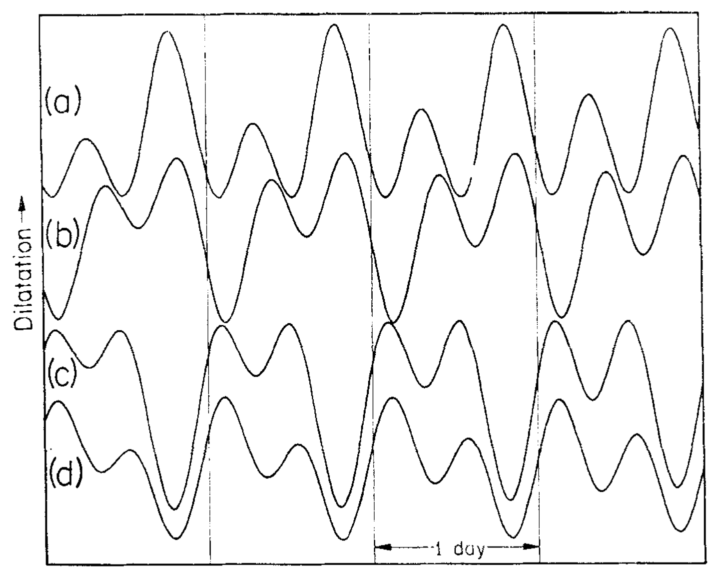

FIG. 7. Tidal volumetric strain assuming an elastic, anisotropic dilatancy type constitutive law. The top curve is a plot of tidal hydrostatic stress as a function of time. The tidal volumetric strain of an isotropic normal crust would be some constant multiple of this curve. The shape and phase of tidal volumetric strain would change if the region of interest were anisotropic, however. The lower three curves show the effect of different orientations of the tectonic co-ordinate system. Here all the curves are plotted for the same tidal stress tensor as a function of time. (a) hydrostatic stress; $(\tau_{11}+\tau_{22}+\tau_{33})/3$; (b) dilatancy volumetric strain for vertical strike-slip earthquake, $\mathbf{e}_1$ dips 0° to NE, $\mathbf{e}_3$ dips 0° to NW; (c) dilatancy volumetric strain for thrust earthquake, $\mathbf{e}_1$ dips to 0° to N, $\mathbf{e}_3$ is vertical; and (d) dilatancy volumetric strain for oblique slip earthquake, $\mathbf{e}_1$ dips 3° towards N36° E, $\mathbf{e}_3$ dips 74° towards S35° E.

to calculate volumetric strain as a function of τ_{11} and τ_{33}. Since tidal stresses are small, this constitutive law can be linearized about any point in stress space. Thus a dilatant region should respond linearly to tidal stress, but the linear response of the material will change in time. Linearization of the constitutive law about a dilatant state would, in general, yield an apparent anisotropy of the dilatant material. If the linearized constitutive law for a dilatant region were anisotropic, one might also expect a shift in phase for certain tidal strains. In fact, for certain fault orientations, dilatancy allows for the possibility of volumetric expansion during tidal compressive hydrostatic stress. Fig. 7 illustrates what the volumetric strain might look like assuming an anisotropic dilatancy constitutive law and several different tectonic co-ordinate frames. It has been assumed in this calculation that the tectonic deviatoric stress $(\tau_{11}-\tau_{33})$, is on the order of 8 kbar with a tectonic confining stress, τ_{33}, of about 1 kbar. The rock would be well within the dilatancy regime for such a high deviatoric stress. In the example of a thrust fault, the $\mathbf{e}_3$ axis is vertical and thus τ_{33} is approximately zero. Results from dilatancy experiments indicate that tidal volumetric expansion should occur when τ_{11} becomes compressive. The constitutive law used for these calculations is not intended to give a true representation of the stress–strain relationships to be expected in the Earth. It merely provides an example of the kinds of phenomena which we might expect to observe in a dilatant region. This example illustrates that there would be not only a change with time in the amplitude of tidal strains due to non-linearity but also, a change with time in the shape and phase of tidal strains due to the apparent anisotropy caused by non-linearity. Modification of tidal strains may already have been observed. Nishimura **(47)** notes that between 1942 and 1946 the strain station at Makimine, Japan recorded variations which seemed to correlate with local earthquakes.

Other problems arise when considering the effect of tides on dilatancy. Experiments by Scholz **(55)** indicate that the stress-strain curve for a dilatant rock is irreversible (non-elastic). That is, the strain depends upon what path the stress has taken. Path dependence most often arises through first and higher order derivatives of the stress path with respect to time. Since tidal stresses occur every day and since their rate of change is probably larger than tectonic stress rates averaged during the dilatancy phase, tides could have a profound effect on the slope of the stress path for any rock which is undergoing dilatancy. Thus the existence of tidal stresses dictates that the hysteresis of a dilatant rock must be examined.

(ii) *Only large earthquakes triggered by tides?*

The argument has been made that tides are important for triggering since the tidal rate of stress change may be larger than the tectonic rate of stress change. The dilatancy-diffusion model adds a new quirk to this reasoning. Diffusion is important in this model since it determines the pore pressure of a rock. The theory is that the confining stress used in any fracture criteria should actually be the effective confining stress $\langle\sigma_{33}\rangle$, which is the true confining stress minus a constant times the pore pressure. The rate of change of the effective confining stress is thus a linear function of the rate of fluid influx to a dilatant region. From the length of the 'anomalistic velocity period' observed for earthquakes of different magnitudes, it has been theorized that the logarithm of the time required for the pore pressure to drop because of dilatancy and then return to normal due to fluid diffusion is a linear function of the earthquakes magnitude (Whitcomb *et al.* **(68)**; Anderson & Whitcomb **(69)**; Scholz *et al.* **(54)**). Thus the rate of change of effective stress depends strongly upon the size of the earthquake. For an earthquake with anomaly periods of several days or less, the rate of change of effective confining stress due to diffusion should completely swamp the rate of stress change due to the tides. For these reasons, earthquakes of magnitude less than three should not correlate with tidal stresses. This immediately suggests an important test for the dilatancy-diffusion model. Small earthquakes which undergo a dilatancy-diffusion process should not be tidally triggered.

Fluid diffusion is not the only model which has been developed to explain the recovery of seismic velocity from anomalously low values to normal prior to an earthquake. Crack closure also appears to adequately explain the present observation of the velocity recovery phase **(9)**. Crack closure essentially postulates that cracks which opened in the dilatancy phase would close again in the velocity recovery phase. The point to be made is that the length of the anomalous period is once again an exponential function of the ensuing earthquake's magnitude (Anderson & Whitcomb **(9)**). It seems inconceivable that small changes in stress due to tides could have a significant effect upon the occurrence time of a small earthquake whose anomalous period is very short, on the order of days. In fact, practically any magnitude dependent deterministic model of earthquakes for which precursor times are of the order of tidal periods would seem to predict that tidal triggering should not occur. Unfortunately, the earthquakes considered in this study are larger than magnitude 4. An important study would be to repeat the process done in this study for small independent dip-slip earthquakes for which V_p anomalies have been observed. There have already been some studies (for instance, see papers by Klein **(29)** and Willis & Taylor **(71)**) which suggest that small earthquakes are tidally triggered. At the present, though, the problem of triggering of small dip-slip earthquakes appears to be unresolved.

Conclusions

Shallow oblique-slip and dip-slip earthquakes whose magnitude is greater than five appear to correlate with tidally generated shear stresses which are sympathetic to failure. This apparent correlation does not seem to be true for strike-slip earthquakes or for any earthquakes which are deeper than 30 km. The dilatancy-diffusion model seems to predict that tidal triggering should not be seen for small magnitude shallow dip-slip earthquakes. A test of the dilatancy-diffusion model is thus suggested by this result.

Acknowledgments

I acknowledge, with thanks, discussions from practically every member of the Seismological Laboratory, particularly Professors Hiroo Kanamori, Don Anderson, C. Hewitt Dix, Clarence Allen and Dr Kunihiko Shimizaki. Dr Henry Fliegel of Jet Propulsion Laboratory wrote the computer subroutines which were used to compute astronomical parameters. Thanks also to Professor Ronald Scott for his comments on fracture processes and Professor Gary Lord for his suggestions concerning statistics. My thanks to Terry Rithaler for typing the paper and L. Lenches for drafting the figures. This research was supported by USGS Contract No. 14-08-0001-14563, and a Jet Propulsion Laboratory Earthquake Prediction Contract.

Division of Geological and Planetary Sciences,
California Institute of Technology,
Pasadena, California 91125.

References

(1) Abe, K., 1972. Mechanisms and tectonic implications of the 1966 and 1970 Peru earthquakes, *Phys. Earth Planet. Int.*, **5**, 367–379.

(2) Abe, K., 1972. Lithospheric normal faulting beneath the Aleutian trend, *Phys. Earth Planet. Int.*, **5**, 190–198.

(3) Adams, R. D., Eiby, G. A. & Lowry, M. A., 1969. A preliminary seismological report (Inangahua earthquake), *Bull. N.Z. Soc. Earthq. Eng.*, **2**, No. 1.

(4) Atshar, H. K., 1968. Report on the Great Dasht-E-Bayaz earthquake of Aug. 31 and Sep. 1, 1968, *Publ. No.* 46, Tehran University Press.

(5) Algermissen, S. T., Dewey, J. W., Langer, C. J. & Dillinger, W. H., 1974. The Managua, Nicaragua, earthquake of December 23, 1972; location, focal mechanism and intensity distribution, *Bull. seism. Soc. Am.*, **64**, 993–1004.

(6) Allen, C. R. & Nordquist, J. M., 1972. Foreshock, main shock, and larger aftershocks of the Borrego mountain earthquake, *Geol. Survey Prof. Paper* **787.**

(7) Allen, M. W., 1936. The lunar triggering of earthquakes in Southern California, *Bull. seism. Soc. Am.*, **26**, 147–157.

(8) Ambraseys, N. N., Zatopek, A., Tasdemiroglu, M. & Aytun, A., 1968. The Modurnu Valley earthquake of 22 July 1967, *Unesco Ser. No.* 622/*BMS, RD/AVS*, Paris.

(9) Anderson, D. L. & Whitcomb, J. H., 1975. Time Dependent Seismology JGR, *Contribution* # 2363, *Div. Geological and Planetary Sciences, Caltech*, in press.

(10) Arroyo, A. L. & Udias, A., 1972. Aftershock sequence and focal parameters of the Feb. 28, 1969 earthquake of the Azores–Gibraltar fracture zone, *Bull. seism. Soc. Am.*, **62**, 699–719.

(11) Beaumont, C. & Berger, J., 1974. Earthquake prediction: modification of the earth tide tilts and strains by dilatancy, *Geophys. J. R. astr. Soc.*, **39**, 111–121.

(12) Brace, W. F., Paulding, B. W. & Scholz, C., 1966. Dilatancy in the fracture of crystalline rocks, *J. geophys. Res.*, **71**, 3939–3953.

(13) Brown, R. D., Vedder, J. G., Wallace, R. E., Roth, E. F., Yerkes, R. F., Castle, R. O., Waananen, A. O., Page, R. W. & Eaton, J. P., 1967. The Parkfield–Cholame California earthquakes of June–August 1966—surface geologic effects, water resources aspects, and preliminary seismic data, *Geological Survey Prof. Paper* **579.**

(14) Chandra, U., 1971. Combination of P & S data for determination of earthquake focal mechanism, *Bull. seism. Soc. Am.*, **61**, 1655–1673.

(15) Cloud, W. K., Hill, D. M., Huffman, M. E., Jennings, C. W., McEvilly, T. V., Nason, R. D., Steinbrugge, K. V., Tucker, J. D., Unger, J. D. & Youd, T. D., 1970. The Santa Rosa earthquake of October, 1969, *Mineral Information Service*, **23**, 43–63.

(16) Dix, C. H., 1964. *Earthquakes and earth tides*, unpublished report, Caltech. See also triggering of some earthquakes, 1964, *Proc. Japan Acad.*, **XL**, 410–415.

(17) Ellsworth, W. L., Cambell, R. H., Hill, D. P., Page, R. A., Alewine, R. W., Hanks, T. C., Heaton, T. H., Hileman, J. A., Kanamori, H., Minster, B. & Whitcomb, J. H., 1973. Point Mugu, California, earthquake of 21 February 1973 and its aftershocks, *Science*, **182**, 1127–1129.

(18) Fukao, Y., 1973. Thrust faulting at a lithospheric plate boundary, the Portugal earthquake of 1969, *Earth Planet. Sci. Lett.*, **18**, 205–216.

(19) Fukao, Y. & Furumoto, M., 1975. Mechanism of large earthquakes along eastern margin of Japan Sea, *Tectonophys.*, in press.

(20) Garg, S. V. & Nur, A., 1973. Effective stress laws for fluid-saturated porous rocks, *J. geophys. Res.*, **78**, 5911–5921.

(21) Gordon, F. R., 1971. Faulting during the earthquake at Meckering, Western Australia; 14 October 1968, *R. Soc. N.Z., Bull.* **9**, recent crustal movements, 85–93.

(22) Groten, E. & Brennecke, J., 1973. Global interaction between Earth and sea tides, *J. geophys. Res.*, **78**, 8519–8526.

(23) Gutenberg, B., 1955. Earthquakes in Kern County, Calif. during 1952, *Calif. Div. Mines Bull.*, **171**, 165–171.

(24) Hamilton, W. L., 1973. Tidal cycles of volcanic eruptions: fortnightly to 19 yearly periods, *J. geophys. Res.*, **78**, 3363–3375.

(25) Isacks, B. & Molnar, P., 1971. Distribution of stresses in the descending lithosphere from a global survey of focal mechanisms of mantle earthquakes, *Rev. Geophys. Space Phys.*, **9**, 103–174.

(26) Kanamori, H., 1971. Seismological evidence for lithospheric normal faulting—the Sanriku earthquake of 1933, *Phys. Earth. Planet. Int.*, **4**, 289–300.

(27) Kanamori, H., 1971. Focal mechanism of Tokachi-Oki earthquake of May 16, 1968, *Tectonophys.*, **12**, 1–13.

(28) Kanamori, H., 1973. Mode of strain release associated with major earthquakes in Japan, *Ann. Rev. Earth Planet. Sci.*, **1**, ed. Fred Donath.

(29) Klein, F. W., 1974. Earthquake swarms and the semidiurnal solid earth tide, EOS, **55**, 551.

(30) Knopoff, L., 1964. Earth tides as a triggering mechanism for earthquakes, *Bull. seism. Soc. Am.*, **54**, 1865–1870.

(31) Knopoff, L., 1970. Correlation of earthquakes with lunar orbital motions, *The Moon*, **2**, 140–143.

(32) Knopoff, L. & Gardner, J. K., 1972. Higher seismic activity during local night on the raw world-wide earthquake catalogue, *Geophys. J. R. astr. Soc.*, **28**, 311–313.

(33) Langdon, J. R. & Thomas, L., 1974. Earth-tide measurements in southeastern Australia, *Bull. seism. Soc. Am.*, **64**, 457–472.

(34) Lawson, A. C., 1908. The California earthquake of April 18, 1906, *Report of the State Earthquake Investigation Commission*, published by Carnegie Inst. of Washington.

(35) Lennon, G. W. & Baker, T. F., 1973. The Earth-tide signal and its coherency, *Geophys J. R. astr. Soc.*, **14**, 161–182.

(36) Louderback, G. D., 1947. Central California earthquakes of the 1830's, *Bull. seism. Soc. Am.*, **37**, 33–75.

(37) Love, A. E. H., 1927. *A treatise on the mathematical theory of elasticity*, fourth edition, Cambridge University Press.

(38) Mauk, F. J. & Johnston, M. J. S., 1973. On triggering of volcanic eruptions by earth tides, *J. geophys. Res.*, **78**, 3356–3362.

(39) Mauk, F. J. & Kienle, J., 1973. Microearthquakes at St. Augustine volcano, Alaska, triggered by earth tides, *Science*, **182**, 386–389.

(40) McKenzie, D., 1972. Active tectonics of the Mediterranean region, *Geophys. J. R. astr. Soc.*, **30**, 109–185.

(41) McMurray, H., 1941. Periodicity of deep-focus earthquakes, *Bull. seism. Soc. Am.*, **31**, 33–56.

(42) Melchior, P., 1966. *The Earth Tides*, Pergamon Press Ltd, Oxford.

(43) Mendiguren, J. A., 1973. Identification of free oscillation spectral peaks for 1970, July 31, Columbian deep shock using the excitation criterion, *Geophys. J. R. astr. Soc.*, **33**, 281–321.

(44) Mikumo, T., 1973. Faulting mechanism of the Gifu earthquake of Sept. 9, 1969 and some related problems, *J. Phys. Earth*, **21**, 191–212.

(45) Morante, E. M. & Allen, C. R., 1973. Displacement on the Philippine fault during the Ragay Gulf earthquake of 17 March 1973, *Geol. Soc. of Am. Abstracts with Programs*, *Vol.* 5, October 1972–1973 Annual Meetings, p. 744.

(46) Murphy, L. M. & Rutlage, J. B., 1959. The Hebgen Lake, Montana, earthquake of August 17, 1959, *Geol. Survey Prof. Paper* **435**, 13–19.

(47) Nishimura, E., 1950. On earth tides, *Trans. Am. geophys. Un.*, **31,** 357–376.

(48) Nowroozi, A. A., 1972. Focal mechanism of earthquakes in Persia, Turkey, West Pakistan, and Afghanistan, and plate tectonics of the Middle East, *Bull. seism. Soc. Am.*, **62,** 823–850.

(49) Rayleigh, Lord, 1919. On the problem of random vibrations and of random flights in one, two, or three dimensions, *Phil. Mag. J. of Sci.*, **37.**

(50) Richter, C. F., 1958. *Elementary seismology*, W. H. Freeman & Company.

(51) Richter, C. F., Allen, C. R. & Nordquist, J. M., 1958. The desert hot springs earthquakes and their tectonic environment, *Bull. seism. Soc. Am.*, **48,** 315–337.

(52) Ryall, A., Van Wormer, J. D. & Jones, A. E., 1968. Triggering of microearthquakes by earth tides, and other features of the Truckee, California earthquake sequences of September, 1966, *Bull. seism. Soc. Am.*, **58,** 215–248.

(53) Sassa, K. & Nishimura, E., 1951. On phenomena forerunning earthquakes, *Trans. Am. geophys. Un.*, **32,** 1–6.

(54) Scholz, C. H., Sykes, L. R. & Aggarwal, Y. P., 1973. The physical basis for earthquake prediction, *Science*, **181,** 803.

(55) Scholz, C. H., Kranz, R., 1974. Notes on dilatancy recovery, *J. geophys. Res.*, **79,** 2132–2136.

(56) Shimazaki, K., 1972. Focal mechanism of a shock at the northwestern boundary of the Pacific plate: extensional feature of the oceanic lithosphere and compressional feature of the continental lithosphere, *Phys. Earth Planet. Int.*, **6,** 397–404.

(57) Shimazaki, K., 1975. Nemuro-Oki earthquake of June 17, 1973: a lithospheric rebound at the upper half of the interface, *Phys. Earth Planet. Int.*, in press.

(58) Shlien, S., 1972. Earthquake-tide correlation, *Geophys. J. R. astr. Soc.*, **28,** 27–34.

(59) Stacey, F. D., 1969. *Physics of the Earth*, John Wiley & Sons, Inc.

(60) Stauder, W. 1968. Tensional character of earthquake foci beneath Aleutian trench with relation to sea-floor spreading, *J. geophys. Res.*, **73,** 3847–3858.

(61) Stauder, W. & Bollinger, G. A., 1966. The focal mechanism of the Alaska earthquake of March 28, 1964 and of its aftershock sequence. *J. geophys. Res.*, **71,** 5283–5296.

(62) Stauder, W., 1973. Mechanism and spatial distribution of Chilean earthquakes with relation to subduction of the oceanic plate *J. geophys. Res.*, **78,** 5033–5061.

(63) Tukeuchi, H., 1951. On the earth tide in the compressible earth of varying density and elasticity, *J. Fac. Sciences, University of Tokyo* Sect. II. Vol. VII, Part 11, 1–153.

(64) Tamrazyan, G. P., 1968. Principal regularities in the distribution of major earthquakes relative to solar and lunar tides and other cosmic sources, *Icarus* **9,** 574–592.

(65) Tasdemiroglu, M., 1971. The 1970 Gediz earthquake in Western Anatolia, Turkey, *Bull seism. Soc. Am.*, **61,** 1507–1529.

(66) Townley, S. D. & Allen, M. W., 1939. Descriptive catalog of earthquakes of the Pacific coast of the United States, 1769 to 1928, *Bull. seism. Soc. Am.*, **29,** 1–297.

(67) Walsh, J. B. & Brace, W. F., 1964. A fracture criterion for brittle anisotropic rock, *J. geophys. Res.*, **69,** 3449–3456.

(68) Whitcomb, J. H., Allen, C. R., Garmany, J. D. & Hileman, J. A., 1973. *Rev. Geophys. Space Phys.*, **11,** 693–730.

(69) Whitcomb, J. H., Garmany, J. D. & Anderson, D. L., 1973. Earthquake prediction: variation of seismic velocities before the San Fernando earthquake, *Science*, **180,** 632–635.

(70) Witkind, I. J., 1959. The Hebgen Lake, Montana, earthquake of August 17, 1959, *Geol. Survey Prof. Paper* **435,** 37–51.

(71) Willis, D. E. & Taylor, R. W., 1974. Investigation of multiple seismic events and first zone discriminants, *ARPA Semi-Annual Technical Report*, April 1974, Caltech.